J. Fluid Mech. (1977), *vol.* 79, *part* 4, *pp.* 801–823
Printed in Great Britain

On a solution of the Lavrentiev wake model and its cascade

By ANCHING LIN
University of Utah, Salt Lake City
AND LOUIS LANDWEBER
Institute of Hydraulic Research, University of Iowa, Iowa City

(Received 16 July 1975 and in revised form 28 May 1976)

A Lavrentiev model of the flow about a blunt two-dimensional body with a separation bubble is considered. Physical bases of the model are discussed in relation to other wake models. The Lavrentiev wake bubble contains a pair of closed free streamlines enclosing the regions of vorticity. It is shown, by means of conformal mapping, that the complex potential can be expressed in terms of elliptic functions, and a one-parameter family of exact solutions has been constructed for a normal flat plate and truncated wedges, for both an unbounded and a bounded stream. A procedure for relating the value of the parameter to the Reynolds number of the real fluid flow is indicated.

1. Introduction

The flow past a bluff object in a uniform stream has long been recognized as one of the unresolved problems in fluid dynamics. The complexity of the problem may be largely attributed to the instability of the flow. At present our capability of treating flow separation in a viscous fluid, even without instability, is far from satisfactory. In the subsequent discussion, we shall confine ourselves to quasi-steady wake flows.

At high Reynolds numbers, the quasi-steady flow around a bluff object may be considered to consist of two regions: one is the boundary layer and the wake, in which the vorticity in the flow is assumed to be concentrated; the other is an outer inviscid irrotational flow. If the body is bluff, usually there will be a near wake or separation bubble, where recirculating flow occurs, and a far wake. Even for this relatively simplified version of the wake flow, there is as yet no satisfactory solution.

There have been numerous experimental investigations of wake flows. We shall discuss some typical results from selected papers which are relevant to the present study. Because of the low level of the mean flow and the high level of the fluctuating flow in a near wake, experimental measurements of the velocity field are difficult. A series of careful measurements carried out with a Pitot tube by Arie & Rouse (1956) revealed some fundamental features of a quasi-steady near wake behind a flat plate. At a Reynolds number of the order of 10^5, the length of the wake bubble is about 17 times the half-width of the plate, and a uniform pressure prevails at the base of the plate, as well as over most of the separation bubble, except in regions close to the reattachment point.

In a series of related papers by Grove *et al.* (1964) and Acrivos *et al.* (1965, 1968), important characteristics of a near wake behind a circular cylinder and bodies of other shapes were presented. Although these experiments were conducted at Reynolds numbers less than 200, their results are similar to those obtained at higher Reynolds numbers. Acrivos *et al.* (1968) found that the base-pressure coefficient for a flat plate reaches a constant value of $-0{\cdot}6$ at a Reynolds number of about 100, in agreement with the value $-0{\cdot}57$ found by Arie & Rouse (1956) at a Reynolds number of about 10^5. It was found that the velocities in most of the near wake are small relative to the free-stream velocity, justifying the term 'dead-water' usually applied to flows in this zone.

Through dimensional considerations, Acrivos *et al.* (1965) also indicated that the length of the near wake should increase linearly with the Reynolds number. This conclusion is obviously not valid for the case of a flat plate; in fact, the length of the near wake measured by Arie & Rouse is of the same order of magnitude as that found by Acrivos *et al.*, in spite of the large difference in Reynolds number. There are insufficient experimental data to ascertain the relation between the size of a wake and the Reynolds number. It appears to be plausible, however, to assume that the length of the near wake approaches a finite limit; at least there are no experimental results contradicting this assumption.

Theoretical treatment of a near wake is inherently difficult, mainly because the wake boundary is not known. Consequently, it is not easy to pose it as a boundary-value problem. Because of the uniform base pressure generally observed behind bluff objects, free-streamline theories have been used as wake models, and a survey of the subject has been given in a review paper by Wu (1972). It was found (Wu, Whitney & Brennan 1971) that free-streamline theory provides a satisfactory representation of liquid flows with cavitation and serves well in predicting wall effects of cavitating flows, but a connexion with viscous effects is not apparent. The limitations of free-streamline theory for the simulation of wake flows were discussed in some detail by Batchelor (1956). For wake flows, one is interested in both the separation and the reattachment, and the influence of the Reynolds number. In dealing with closed wakes, the open-cavity model is apparently of limited use. Finite-cavity models, such as that of Riabouchinsky and the re-entrant-jet model, are unrealistic as far as the re-attachment process is concerned.

Free-streamline theory gains its popularity for wake-flow representation mainly through the fact that, once the base pressure is prescribed, the form drag can be calculated accurately with either of the aforementioned models. The exploitation of this property merely emphasizes the point that potential-flow theory could play an important role in the analysis of wake flow at high Reynolds numbers, but no insight is provided regarding the physical mechanism of the viscous flows in the near wake.

Batchelor (1956) proposed a closed near-wake model which consists of uniformly distributed vorticity and a cusped closure for the wake; no specific

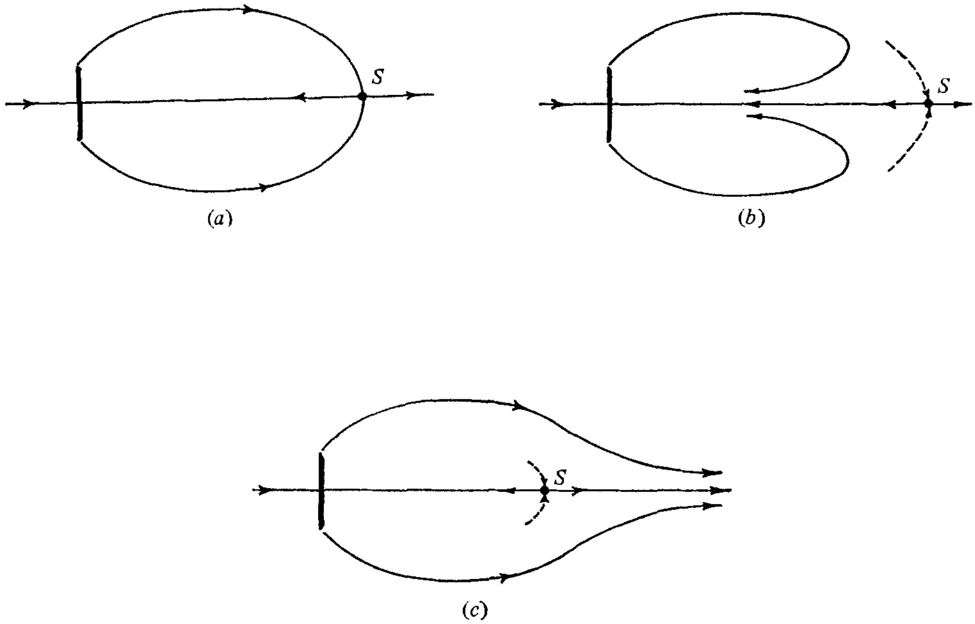

FIGURE 1. Possible dividing streamlines. (*a*) Closed. (*b*) Re-entrant. (*c*) Open.

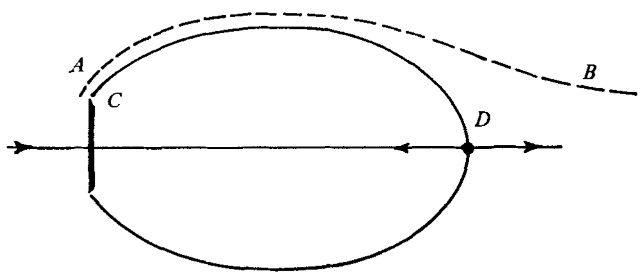

FIGURE 2. Streamlines *AB* and *CD*.

solutions, however, were given for the model, which is concerned with the limiting conditions at very high Reynolds numbers. The model assumes that viscous effects are concentrated along the boundary of the near wake, which becomes a singular surface as the Reynolds number tends to infinity. Tacitly, then, the model presupposes that the flow within the near wake is inviscid as the Reynolds number approaches infinity.

In mathematical models of the near wake, the streamline emanating from the point of separation serves as the delineating boundary between the recirculating near wake and the outer flow. Sketches of three possible ways in which the dividing streamline may behave are shown in figure 1. We refer to this streamline as the boundary of the wake or separation bubble. That depicted in figure 1 (*a*) reattaches at a stagnation point. The re-entrant jet type is shown in figure 1 (*b*) and the type open at the rear in figure 1 (*c*). The last two types are not possible models, since the former implies a fluid sink and the latter, a fluid source within the separation bubble.

Lavrentiev (1962, p. 47) briefly sketched a possible wake model of the type shown in figure 1 (*a*) which consists of a pair of closed free streamlines, as shown in figure 3. Two options were suggested for the construction of the wake model: to treat the flow in the region between the boundary of the near wake and the closed free streamline either as rotational or as irrotational. The one-paragraph description of the model was very brief, and no solutions were given nor was a physical basis for the model indicated.

We note that, at high but finite Reynolds numbers, a distinction between two specific lines must be made. In figure 2, the line AB represents the outer boundary layer and wake, while CD is the dividing streamline, discussed in the preceding paragraph, which terminates at the stagnation point D. In physical terms, the dividing streamline CD in Lavrentiev's wake and Batchelor's cusped limiting streamline AB for infinite Reynolds number are not the same. As the Reynolds number increases indefinitely, the two are expected to approach each other, however, according to Batchelor.

Of Lavrentiev's two proposed models, that with vorticity between the wake bubble and the outer boundary of the wake is more realistic but a model with irrotational flow outside the wake bubble can also yield useful information, and in addition has the important advantage that an exact analytical solution can be derived. One may object that this irrotational-flow model gives zero drag for the blunt body; but so does the irrotational-flow pressure distribution about a slender body, which is used to obtain the pressure gradients for a calculation of the boundary layer on that body. If the boundary layer is still thin at the separation point, the pressure distribution given by the Lavrentiev irrotational model could similarly serve as a first approximation for developing his rotational model. Perhaps even more useful is the fact that the pressure at the separation point given by the irrotational model can be used to calculate the drag if the experimental result that the pressure is constant on the surface of the body within the separation bubble is applied.

In common with other wake models, that of Lavrentiev yields a one-parameter family of wake bubbles which, if possible, should be correlated with the Reynolds number. Unlike other wake models, the irrotational Lavrentiev model can be so correlated, as will be indicated.

The authors' interest in this problem originated from an attempt to explain the large observed effect of channel walls on the drag of a blunt body (Lin 1966; Landweber 1970) in terms of the dimensions of the separation bubble. The Lavrentiev irrotational model was preferred and developed (Lin 1970), although, at the time, the authors were unaware of Lavrentiev's proposals.

The purpose of this paper is to present a mathematical solution of the Lavrentiev irrotational model, both without and with walls. The solution is based on Riemann's theorem on canonical mapping, the Schwarz reflexion principle, and on the elegant theory of Weierstrass elliptic functions. It should be noted that these ideas were presented and exploited in great detail by Sedov (1965, p. 213) in his treatise on two-dimensional flow problems.

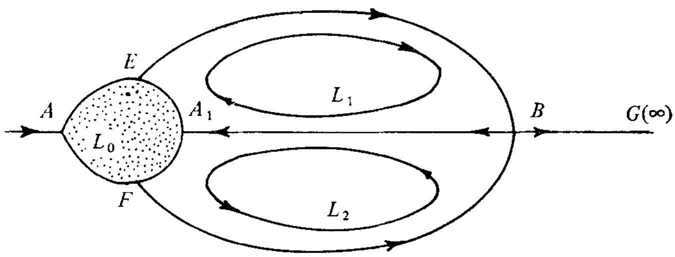

FIGURE 3. A Lavrentiev model for an arbitrary symmetric blunt body.

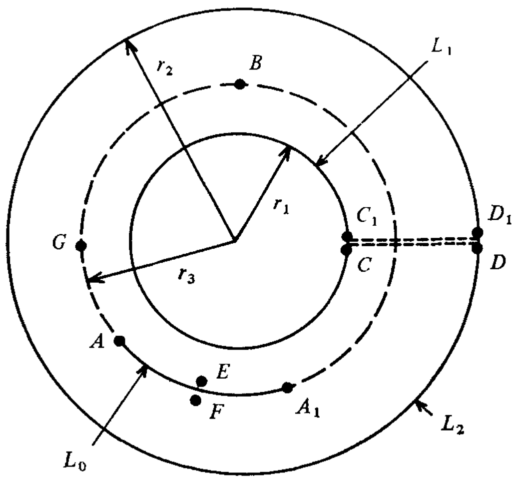

FIGURE 4. ξ plane.

2. Plan of analysis

The general plan of the analysis is to construct the solution on a parametric plane in the following steps:

(i) Map the entire physical (z) plane onto a rectangular region in a parametric (u) plane. The case without confining walls is treated first.

(ii) Establish the double periodicity in the parametric plane of dW/du and dW/dz, where W is the complex potential.

(iii) Derive specific forms for dW/du as a function of u for a symmetric object of arbitrary shape.

(iv) Derive specific forms for dW/dz as a function of u for a flat plate and wedges.

(v) Specify conditions for the determination of mapping parameters.

(vi) Derive the solution for the general case of flow past wedges.

(vii) Obtain the solution for the cascade problem for a flat plate by the same procedure, i.e. steps (i)–(v). For the cascade problem, an infinite strip, instead of the entire z plane, is mapped onto a rectangular region.

(viii) The solution of the cascade problem for wedges can be obtained similarly, although a detailed solution is not presented here.

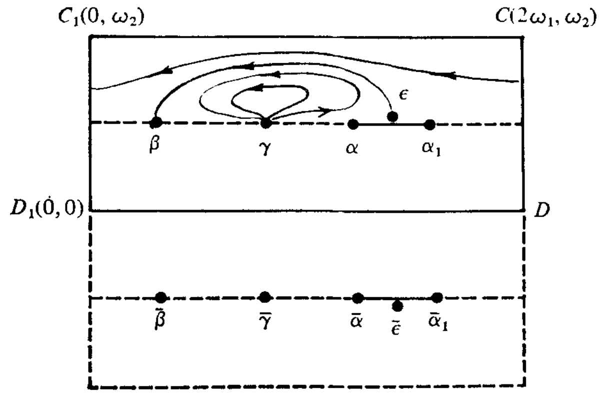

FIGURE 5. Parametric (u) plane.

3. The physical (z) plane and the parametric (u) plane

Consider a two-dimensional, symmetric, potential flow in the z plane past a symmetric obstacle L_0 with a separation pocket EBF inside which there are two symmetric closed curves L_1 and L_2 which will be taken as free, constant-pressure streamlines. The x axis will be taken as the axis of symmetry; see figure 3. Then L_0, L_1 and L_2 are contours enclosing three separate regions, of which that inside L_0 is given but the shapes of L_1 and L_2 are initially unknown. In figure 3, A, A_1 and B are stagnation points, and the closed curve $EBFA_1E$ bounds the separation pocket.

In the following two steps, the physical plane will be mapped into a parametric u plane where L_1 and L_2 have a known shape.

3.1. *Canonical annular region in ξ plane*

By the theorem of canonical mappings (Nehari 1952), the triply connected physical plane can be mapped one-to-one into an annular region in a ξ plane; see figure 4. L_1 and L_2 are mapped into concentric circles of radii r_1 and r_2 in the ξ plane and L_0 is mapped into a concentric circular arc AA_1 of radius r_3. Infinity in the z plane is mapped into the point G in the ξ plane. We may choose the mapping such that B and G lie on the same circle as AA_1. The radii satisfy the relation

$$r_1 r_2 = r_3^2, \tag{1}$$

as is seen by applying the Schwarz reflexion principle to the line segment A_1BGA in the z plane and the corresponding circular arc in the ξ plane.

3.2. *The parametric (u) plane*

If a radial cut CD (or C_1D_1) is introduced, the annular region in the ξ plane is mapped one-to-one into a rectangular region $C_1D_1DCC_1$ in the u plane, shown in figures 5 and 6, by

$$u = -\frac{i\omega_1}{\pi}\ln\frac{\xi}{r_1}, \quad \xi = r_1 \exp\frac{\pi i u}{\omega_1}, \tag{2}$$

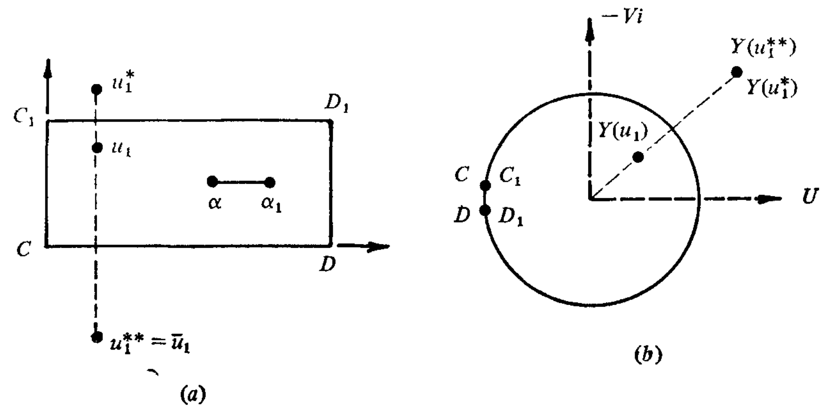

FIGURE 6. Mapping $Y = Y(u)$. (a) u plane. (b) Y plane.

where ω_1 is real. We define the imaginary number ω_2 by

$$\omega_2 = u(r_2) = -\frac{i\omega_1}{\pi}\ln\frac{r_2}{r_1}. \tag{3}$$

Then, in figure 4 we have $D_1 D = 2\omega_1$ and $DC = |\omega_2|$. The Schwarz reflexion principle then shows that the circle L_0 in the ξ plane maps into a parallel line midway between $D_1 D$ and $C_1 C$ in the u plane, along which lie the points β, γ, α, ϵ and α_1, the images of B, G, A, E and A_1. We may choose $\omega_1 = 1$ and

$$u(D_1) = (0,0), \quad u(D) = (2,0), \quad \gamma = 1 + \tfrac{1}{2}\omega_2. \tag{4a–c}$$

Equations (4) exhaust the three degrees of freedom available to a conformal mapping. The remaining parameters must be determined by other conditions which will be considered subsequently.

4. Periodicities of dW/du and dW/dz on the parametric (u) plane

Let $W = \phi + i\psi$ denote the complex potential, where ϕ is the velocity potential and ψ the stream function. We shall show that dW/du and dW/dz are doubly periodic.

By (2), we have $\xi(u) = \xi(u + 2\omega_1)$. Since $z = f(\xi)$, this yields

$$z(u + 2\omega_1) = z(u), \tag{5}$$

i.e. $z(u)$ is periodic with period $2\omega_1$. Then we also have

$$W[z(u)] = W[z(u + 2\omega_1)] \tag{5a}$$

and

$$dW(u)/dz = dW(u + 2\omega_1)/dz, \tag{6}$$

i.e. $dW(u)/dz$ is periodic with period $2\omega_1$. This implies that dW/du is also periodic with period $2\omega_1$, since $dW/du = (dW/dz)\,(dz/du)$.

Next we observe that $\psi = -\psi_0$, 0 and ψ_0 along $C_1 C$, GA and $D_1 D$ respectively, where ψ_0 is a constant. Then, applying the Schwarz reflexion principle successively

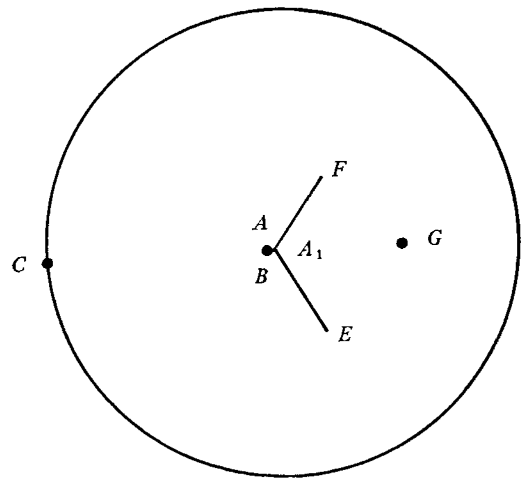

FIGURE 7. Hodograph plane for flow past a wedge.

to GA and C_1C in the u plane, and to the corresponding line segments in the W plane, we obtain

$$W(u+\omega_2) = W(u)-2i\psi_0$$

and hence $$dW(u)/du = dW(u+\omega_2)/du. \tag{7}$$

Lastly, we shall show that $Y = dW/dz$ is periodic with period $2\omega_2$. For this we employ the condition that $|Y|$ = constant along C_1C and D_1D, so that C_1C and D_1D in the u plane map into the same circle in the hodograph plane $Y = U-iV$. Then, by the Schwarz reflexion principle, mirror images u^* and u^{**} in C_1C and D_1D of a point u yield $Y(u^*) = Y(u^{**})$. But, as is readily verified,

$$u^* = u^{**}+2\omega_2$$

and hence, dropping the superscripts,

$$dW(u)/dz = dW(u+2\omega_2)/dz. \tag{8}$$

Clearly the mapping $Y(u)$ is not one-to-one; it is, however, single-valued, which is all that is required. The above arguments are demonstrated schematically in figure 6; a hodograph for a wedge is shown in figure 7.

5. Construction of dW/du

We have shown that dW/du is doubly periodic with periods $2\omega_1$ and ω_2. For large values of $|z|$, the complex velocity may be expressed in the form

$$dW/dz = U+C_2/z^2+\dots,$$

where U is the free-stream velocity. Because $z(u)$ has a pole of first order at $u = \gamma$, in the neighbourhood of $u = \gamma$ we can write

$$z(u) = k/(u-\gamma)+k_0+k_1(u-\gamma)+\dots. \tag{9}$$

Hence we obtain

$$\frac{dW}{dz} = U + \frac{C_2}{k^2}(u-\gamma)^2 + \ldots \tag{10}$$

and

$$\frac{dW}{du} = \frac{dW}{dz}\frac{dz}{du} = -\frac{kU}{(u-\gamma)^2} + a_0 + a_1(u-\gamma) + \ldots, \tag{11}$$

i.e. dW/du has a pole of second order at $u = \gamma$.

Furthermore, there are no other singular points of $W(z)$ outside the given obstacle L_0 and the hollow vortices L_1 and L_2. The fact that dW/du is regular at $u = \alpha$ or α_1 may be demonstrated as follows. Since α is a branch point of order 1 for a blunt body, we have in the neighbourhood of $z = z_A$

$$u-\alpha = C_2(z-z_A)^2 + C_3(z-z_A)^3 + \ldots, \quad du/dz = 2C_2(z-z_A) + \ldots$$

and

$$dW/dz = k(z-z_A) + \ldots .$$

Thus

$$\frac{dW}{du} = \frac{dW}{dz}\frac{dz}{du} = \frac{k(z-z_A)+\ldots}{2C_2(z-z_A)+\ldots}$$

and hence dW/du is regular at $u = \alpha$, and similarly at $u = \alpha_1$. A similar proof may be given for the case where A is a corner point.

We have now seen that dW/du is meromorphic and doubly periodic. Hence it is an elliptic function of order 2, which may be written in the form

$$dW/du = kU[Q - P(u-\gamma;\quad 2\omega_1, \omega_2)], \tag{12}$$

where $P(u-\gamma;\, 2\omega_1,\, \omega_2)$ is the Weierstrass *Pe* function with periods $2\omega_1$ and ω_2, and Q and k are undetermined constants. dW/du is readily integrated to yield

$$W(u) = kU[Qu + \zeta(u-\gamma; 2\omega_1, \omega_2) + Q_0], \tag{13}$$

where $\zeta(u-\gamma;\, 2\omega_1,\, \omega_2)$ is the Weierstrass zeta function with quasi-periods $2\omega_1$ and ω_2, and Q_0 is a constant. This expression suggests that we can interpret the extended u plane as a flow field with a free-stream velocity Q passing through a cascade of doublets located at $u = \gamma$ and its congruent points $\gamma + 2m\omega_1 + n\omega_2$ $(m, n = \pm 1, \pm 2, \pm 3, \ldots)$. See the sketch of streamlines in the u plane, figure 5.

Let us recall that the streamlines passing through points B and E in the z plane form the boundary of a flow pocket. We may then state that, in the period rectangle, the closed streamline passing through β and ϵ divides the flow into two distinct regions, one with streamlines originating and terminating at $u = \gamma$, and the other with streamlines without any direct geometric connexion with the point $u = \gamma$. The latter corresponds, in the z plane, to the region enclosed in the pocket A_1EBFA_1, and the former to the rest of the flow region. In order to accomplish this division, β and ϵ in the u plane must be taken as stagnation points, and hence are the two zeros of the elliptic function (12), associated with the pole of second order at $u = \gamma$. The theory of elliptic functions then requires the relation

$$\epsilon + \beta = 2\gamma \tag{14}$$

to hold, and the condition that β is a zero of dW/du gives the value of Q:

$$Q = P(\beta - \gamma; 2\omega_1, \omega_2). \tag{14a}$$

6. Flow past a flat plate

The foregoing derivation of dW/du is for flows past arbitrary symmetric obstacles. An expression for dW/dz is also required to complete a solution. This will now be constructed for the case of a flat plate.

6.1. *Construction of dW/dz and dz/du*

It has been shown that dW/dz is periodic with periods $2\omega_1$ and $2\omega_2$. The nature of the zeros and singularities of dW/dz will now be investigated. For a flat plate, A, A_1 and B are the only stagnation points in the z plane, and hence these points are simple zeros of dW/dz. Then, since $u = \alpha$ is a branch point of $z(u)$ of order 1, we have

$$dW/dz = a_1(u-\alpha)^{\frac{1}{2}} + a_2(u-\alpha) + \dots. \tag{15}$$

Similarly, in the neighbourhood of α_1,

$$dW/dz = b_1(u-\alpha_1)^{\frac{1}{2}} + b_2(u-\alpha_1) + \dots. \tag{16}$$

On the other hand, since $z(u)$ is single-valued at $u = \beta$, we have

$$dW/dz = C_1(u-\beta) + C_2(u-\beta)^2 + \dots. \tag{17}$$

We shall now show that dW/dz is singular at $u = \overline{\alpha}$, $\overline{\alpha}_1$ and $\overline{\beta}$, the complex conjugates of α, α_1 and β. The proof is based on the Schwarz reflexion principle, applied to the line $D_1 D$ in the u plane and the corresponding circle of radius $\lambda = |dW/dz|$ in the hodograph plane $Y = dW/dz$. Mirror images in $D_1 D$ then become inverse points relative to the circle and we have $Y(\overline{u}) = \lambda^2/Y(u)$. This indicates that $\overline{\alpha}$ and $\overline{\alpha}_1$ are singular points, and branch points of order 1, while $\overline{\beta}$ is a simple pole of dW/dz.

Now consider the expression

$$\frac{dW}{dz} = C_0 \exp(i\delta) \left(\frac{\sigma(u-\alpha)\,\sigma(u-\alpha_1)}{\sigma(u-\overline{\alpha}_1)\,\sigma(u-\overline{\alpha}_1)}\right)^{\frac{1}{2}} \frac{\sigma(u-\beta)}{\sigma(u-\overline{\beta})} \exp(2\eta_2 u), \tag{18}$$

where $\sigma(u)$ is the Weierstrass sigma function, with quasi-periods $2\omega_1$ and $2\omega_2$ understood, C_0 and δ are real constants, and $\eta_2 = \zeta(\omega_2;\, 2\omega_1, 2\omega_2)$. We note that η_2 is imaginary when ω_1 is real and ω_2 imaginary, as in the present case (Abramowitz & Stegun 1964, p. 633). Another form for dW/dz is

$$\frac{dW}{dz} = \frac{C}{[P(u-\alpha)-e_2]^{\frac{1}{2}}[P(u-\alpha_1)-e_2]^{\frac{1}{2}}[P(u-\beta)-e_2]^{\frac{1}{2}}} \equiv \frac{C}{\Pi(u)}, \tag{18a}$$

where $e_2 = P(\omega_2)$, and the complex number

$$C = [C_0/\sigma^2(\omega_2)] \exp\{\eta_2(\tfrac{1}{2}\alpha + \tfrac{1}{2}\alpha_1 + \beta) + i\delta\} \tag{19}$$

can be derived from (18) by means of the relation (Dutta & Debnath 1965, p. 73)

$$\sigma(u-\overline{\alpha})/\sigma(u-\alpha) = \sigma(\omega_2) \exp[\eta_2(u-\alpha)]\,[P(u-\alpha)-e_2]^{\frac{1}{2}} \tag{20}$$

and similar expressions in α_1 and β. Here the Weierstrass *Pe* functions have periods $2\omega_1$ and $2\omega_2$, in contrast with those for dW/du in (12). It is apparent, then, from (18*a*) that the form for dW/dz has the required periods $2\omega_1$ and $2\omega_2$. Furthermore, since $\sigma(u)$ has a first-order zero at $u = 0$, we see that (18) has zeros at α, α_1 and β, a pole at $\bar{\beta}$, and singular points $\bar{\alpha}$ and $\bar{\alpha}_1$ with the desired type of branching.

We must also show that the normal flat plate is a streamline, or, equivalently, that $\arg dW/dz$ is constant for points u on the line segment between α and α_1, i.e. for $u = \alpha + t(\alpha_1 - \alpha)$, $0 \leqslant t \leqslant 1$. This may be proved by observing that, when ω_1 is real and ω_2 is imaginary, the *Pe* function is real for real values of its argument and e_2 is also real (Dutta & Debnath 1965, p. 40). Hence, since $u-\alpha$, $u-\alpha_1$ and $u-\beta$ are real for values of u on $\alpha\alpha_1$, $P(u-\alpha)-e_2$, $P(u-\alpha_1)-e_2$ and $P(u-\beta)-e_2$ are also real. Nor can these factors vanish in the above interval since the only zeros of $P(u)-e_2$ occur at $u = \omega_2$ (Whittaker & Watson 1950, p. 443). Hence, for these values of u, $\arg[dW/dz]$ is constant, as we wished to show. Thus the expression for dW/dz in (18) or (18*a*) appears to be suitable for the flow about a normal plate.

Since L_1 and L_2 are free streamlines, dW/dz along L_1 and L_2 must have a constant modulus. We shall now show that (18) satisfies this condition. We note that η_2 is imaginary and that $\sigma(\bar{z}) = \overline{\sigma(z)}$ (Abramowitz & Stegun 1964, p. 631). Then, along L_2, where u is a real number,

$$\left|\frac{\sigma(u-\alpha)}{\sigma(u-\bar{\alpha})}\right| = \left|\frac{\sigma(u-\alpha)}{\overline{\sigma(u-\alpha)}}\right| = 1,$$

with similar results involving α_1 and β; hence $|dW/dz| = C_0$. By using the sigma-function identity

$$\sigma(u+2\omega_i) = -\sigma(u)\exp[2\eta_i(u+\omega_i)], \quad \eta_i = \zeta(\omega_i; 2\omega_1, 2\omega_2) \quad (i = 1, 2),$$

one can similarly establish that $|dW/dz| = C_0$ along L_1.

The function $z(u)$ may now be obtained from

$$z(u) = \int_\alpha^u F(u)\,du, \tag{21}$$

where $F(u) = (dW/du)/(dW/dz)$ is given by (12) and (18). We note that $z(u)$ has a branch point of order 1 at $u = \epsilon$, but is regular at $u = \beta$. The former property may be demonstrated by observing that $dW/du = 0$, $dW/dz \neq 0$ and hence $dz/du = 0$ at $u = \epsilon$. Then

$$z - z_E = m_2(u-\epsilon)^2 + m_3(u-\epsilon)^3 + \dots.$$

On the other hand, $u = \beta$ is a regular point, since β is a simple zero of both dW/du and dW/dz.

6.2. *Determination of parameters*

Except for the three conditions (4*a*–*c*), the parameters defining the mapping remain unspecified. In order to satisfy properties of mapping functions appropriate to the present problem, the parameters must be interrelated in a specific manner. The following conditions need to be imposed.

Velocity at infinity. Equating the Taylor expansion of dW/dz about $u = \gamma$ in (18a) to its asymptotic form given in (10), we obtain

$$U + (C_2/K)(u-\gamma)^2 \simeq C\{1 - \tfrac{1}{4}(u-\gamma)\,S(\gamma)\}/\Pi(\gamma),$$

where
$$S(\gamma) = \frac{P'(\gamma-\alpha)}{P(\gamma-\alpha)-e_2} + \frac{P'(\gamma-\alpha_1)}{P(\gamma-\alpha_1)-e_2} + \frac{2P'(\gamma-\beta)}{P(\gamma-\beta)-e_2} \tag{22}$$

and $P'(u)$ denotes dP/du. Put

$$\alpha = a + \tfrac{1}{2}\omega_2, \quad \alpha_1 = a_1 + \tfrac{1}{2}\omega_2, \quad \beta = b + \tfrac{1}{2}\omega_2, \quad \gamma = 1 + \tfrac{1}{2}\omega_2.$$

Then, since U is real, equating the first terms of the expansions and applying (19) yields

$$i\delta + \tfrac{1}{2}\eta_2(a + a_1 + 2b) = 0, \tag{23}$$

and since (Abramowitz & Stegun 1964, p. 633)

$$\sigma^2(\omega_2) = -[2e_1^2 + 5e_1e_2 + 2e_2^2]^{-\frac{1}{2}} \exp(\eta_2\omega_2), \quad e_1 = P(1), \tag{24}$$

from (19) and (23) we obtain

$$C = -C_0[2e_1^2 + 5e_1e_2 + 2e_2^2]^{\frac{1}{2}} = U\Pi(\gamma). \tag{25}$$

We also see that the linear term in $u-\gamma$ must vanish. This gives

$$S(\gamma) \equiv \frac{P'(1-a)}{P(1-a)-e_2} + \frac{P'(1-a_1)}{P(1-a_1)-e_2} + \frac{2P'(1-b)}{P(1-b)-e_2} = 0. \tag{26}$$

Periodicity of $z(u)$. We have seen in (5) that $z(u)$ is periodic with period $2\omega_1$. According to its definition, $F(u)$ is also periodic with period $2\omega_1$. We then have

$$z(u+2\omega_1) = \int_\alpha^{u+2\omega_1} F(u)\,du = \int_\alpha^{\alpha+2\omega_1} F(u)\,du + \int_{\alpha+2\omega_1}^{u+2\omega_1} F(u)\,du.$$

In the last integral let us change the variable to $u' = u - 2\omega_1$. We then obtain

$$\int_{\alpha+2\omega_1}^{u+2\omega_1} F(u)\,du = \int_\alpha^u F(u'+2\omega_1)\,du' = \int_\alpha^u F(u')\,du' = z(u).$$

Hence the condition $z(u+2\omega_1) = z(u)$ is equivalent to

$$\int_\alpha^{\alpha+2\omega_1} F(u)\,du = 0. \tag{27}$$

Here, from (12) and (18a), $F(u)$ is given by

$$F(u) = (kU/C)\,[Q - P(u-\gamma; 2, \omega_2)]\,\Pi(u). \tag{28}$$

Let us take as the path of integration the horizontal line $\beta\gamma\alpha\alpha_1$, avoiding the point γ by a small semicircle with γ as centre which makes a zero contribution to the integral. Put $u = \mu + \tfrac{1}{2}\omega_2$, $0 \leqslant \mu \leqslant 2\omega_1 = 2$. We see that $F(u)$ is real for $0 \leqslant \mu \leqslant a$ and $a_1 \leqslant \mu \leqslant 2$, but imaginary for $a \leqslant \mu \leqslant a_1$. Hence (27) yields the pair of equations

$$\int_{\alpha_1-2}^{\alpha} F(u)\,du = 0, \quad \int_\alpha^{\alpha_1} F(u)\,du = 0. \tag{29a, b}$$

Although the path of integration of the first of these integrals passes through the singular point γ, it can be evaluated by treating the integrand as a generalized function (Lighthill 1960, p. 16).

Width of the flat plate. We may normalize distance such that the plate is two units wide. This gives $z(\epsilon) = i$, or from (21),

$$\int_{\alpha}^{\epsilon} F(u)\,du = i. \tag{30}$$

6.3. *Summary of equations*

For a flat plate in an unbounded stream, the complex potential has been expressed in terms of a parameter u by means of the equations

$$W(u) = kU[\zeta(u-\gamma; 2, \omega_2) + Qu + Q_0], \tag{13}$$

$$z(u) = \int_{\alpha}^{u} F(u)\,du, \tag{21}$$

$$F(u) = kU[Q - P(u-\gamma; 2, \omega_2)]\,\Pi(u)/C, \tag{28}$$

$$Q = P(\beta-\gamma; 2, \omega_2), \tag{14}$$

$$C = -C_0(2e_1^2 + 5e_1 e_2 + 2e_2^2)^{\frac{1}{2}} = U\Pi(\gamma). \tag{25}$$

For determining the five constants ω_2, k, a, a_1 and b, we have the following four equations:

$$S(\gamma) = 0, \tag{26}$$

$$\int_{\alpha_1-2}^{\alpha} F(u)\,du = 0, \quad \int_{\alpha}^{\alpha_1} F(u)\,du = 0, \tag{29a, b}$$

$$\int_{\alpha}^{\epsilon} F(u)\,du = i \quad (\epsilon = 2\gamma-\beta). \tag{30}$$

This indicates that there exists a one-parameter family of solutions.

In order to obtain numerical solutions, it is convenient to take ω_2 as the free parameter. For a given value of ω_2, the equations can be solved for the other constants by an iterative procedure. Let a_n, a_{1n} and b_n denote an approximate solution of (26) and (29a, b), and put

$$a_{n+1} = a_n + \Delta a, \quad a_{1,n+1} = a_{1n} + \Delta a_1, \quad b_{n+1} = b_n + \Delta b.$$

Then, expanding (26) in a Taylor series, we obtain

$$S(\gamma)_n = \frac{\partial S(\gamma)}{\partial a_n}\Delta a + \frac{\partial S(\gamma)}{\partial a_{1n}}\Delta a_1 + \frac{\partial S(\gamma)}{\partial b_n}\Delta b = 0.$$

Also, from the Taylor expansion of $F(u)$, we obtain

$$\int_{\mu} F_n(u)\,du + \left[F_n(a_n) + \int_{\mu}\frac{\partial F_n}{\partial a_n}du\right]\Delta a + \left[-F_n(a_{1n}) + \int_{\mu}\frac{\partial F_n}{\partial a_{1n}}du\right]\Delta a_1$$
$$+ \Delta b \int_{\mu}\frac{\partial F_n}{\partial b_n}du = 0, \quad \text{with} \quad \int_{\mu} = \int_{\alpha_{1n}-2}^{\alpha_n},$$

and

$$\int_\nu F_n(u)\,du + \left[-F_n(a_n) + \int_\nu \frac{\partial F_n}{\partial a_n}\,du\right]\Delta a + \left[F_n(a_{1n}) + \int_\nu \frac{\partial F_n}{\partial a_{1n}}\,du\right]\Delta a_1$$

$$+\Delta b \int_\nu \frac{\partial F_n}{\partial b_n}\,du = 0, \quad \text{with} \quad \int_\nu = \int_{\alpha_n}^{\alpha_{1n}}.$$

Here $F_n(u)$ denotes $F(u;\, a_n,\, a_{1n},\, b_n)$. The solution of this set of linear equations yields values of Δa, Δa_1 and Δb, and hence values of a_{n+1}, $a_{1,n+1}$ and b_{n+1}.

6.4. *Some flow characteristics*

These results can be immediately applied to derive expressions for the circulation and stream function of the free streamlines. The circulation is given by the change in the complex potential along $D_1 D$, which, by (12), yields

$$\Gamma = W(2) - W(0) = 2Q + kU[\zeta(2-\gamma) - \zeta(-\gamma)]$$
$$= 2Q + 2kU\eta_1(2\omega_1, \omega_2) \tag{31}$$

since (Abramowitz & Stegun 1964, p. 631)

$$\zeta(u+2\omega_1) = \zeta(u) + 2\eta_1, \quad \eta_1 = \zeta(\omega_1;\, 2\omega_1, \omega_2). \tag{32}$$

Let us take $\psi = 0$ as the value of the stream function on the axis of symmetry. Since the velocity potentials at corresponding points on the free streamlines are equal, we can obtain the stream function ψ_0 on the free streamline L_1, or $C_1 C$, from the difference in the complex potentials. Applying (13), we find

$$i\psi_0 = \tfrac{1}{2}[W(\omega_2) - W(0)] = \tfrac{1}{2}Q\omega_2 + \tfrac{1}{2}kU[\zeta(\omega_2-\gamma) - \zeta(-\gamma)]$$
$$= \tfrac{1}{2}Q\omega_2 + kU\eta_2, \quad \eta_2 = \zeta(\tfrac{1}{2}\omega_2;\, 2\omega_1, \omega_2), \tag{33}$$

in which the formula corresponding to (32) for the period ω_2 has been applied.

As was remarked in the introduction, the drag on the body, with the assumed closed wake and the interior constant-pressure streamlines, must be zero, since the force on the constant-pressure streamlines is zero and the drag on the combination of the body and the closed wake is zero. A drag can be determined, however, by using the pressure distribution on the body up to the separation point E, and assuming that the pressure on the portion of the body surface within the separation bubble is constant and equal to the pressure at E. The drag D on the flat plate would then be given by

$$D = 2\int_A^E (p - p_E)\,dy = i\rho \int_A^E v^2 dz + \rho v_E^2,$$

where v is the magnitude of the velocity along the plate, i.e. $v = i\,dW/dz$, and ρ is the mass density of the fluid. Hence we obtain

$$D = \rho \left|\frac{dW}{dz}\right|_E^2 - \rho \int_\alpha^\epsilon \left|\frac{dW}{dz}\right| \frac{dW}{du}\,du, \tag{34}$$

where dW/du and dW/dz are given in (12) and (18).

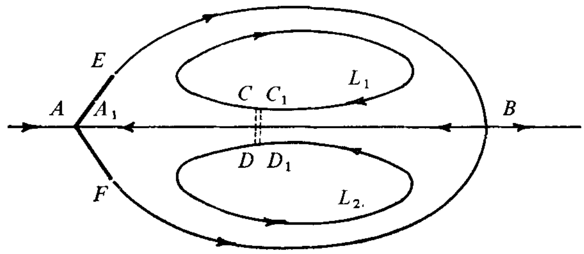

FIGURE 8. Lavrentiev model for a wedge of angle $2\pi/n$.

7. Flow past wedges

The previously derived expressions (12) and (13) for dW/du and $W(u)$ are applicable to arbitrary symmetric obstacles, and hence to the case of a symmetrically situated wedge. Let $2\pi/n$ denote the interior angle of the wedge, shown in figure 8.

The form of dW/dz as a function of u for a wedge is also doubly periodic in the u plane, with periods 2 and $2\omega_2$, and hence its specification depends only upon the nature of its zeros and singularities. Again, the zeros of dW/dz occur at α, α_1 and β and its singularities are situated at the complex conjugates $\bar{\alpha}$, $\bar{\alpha}_1$ and $\bar{\beta}$. As before, dW/dz has a simple zero at $u = \beta$ and a simple pole at $\bar{\beta}$.

For exterior flow about the wedge, one can readily verify that the complex potential

$$W(z) = b_0(z-z_A)^{n/(n-1)}+\ldots$$

gives the desired branching of the streamline $\psi = 0$ from GA to AE in the neighbourhood of z_A. Also, since the exterior angle $2\pi(n-1)/n$ at z_A is transformed into 2π at α, we have

$$z-z_A = k_0(u-\alpha)^{1-1/n}+\ldots.$$

We obtain, then, for $u \approx \alpha$,

$$\frac{dW}{dz} = \frac{b_0 n}{n-1}(z-z_A)^{1/(n-1)}+\ldots = \frac{b_0 n}{n-1}(u-\alpha)^{1/n}+\ldots.$$

Similarly, for interior flow in the wedge, in the neighbourhood of A_1 we obtain

$$dW/dz \sim (u-\alpha_1)^{1-1/n}.$$

Near $\bar{\alpha}$ and $\bar{\alpha}_1$ we then have

$$dW/dz \sim (u-\bar{\alpha})^{-1/n}, \quad dW/dz \sim (u-\bar{\alpha}_1)^{-1+1/n}.$$

A form for dW/dz with the desired characteristics is then

$$\frac{dW}{dz} = K_0 \exp(i\delta)\left\{\frac{\sigma(u-\alpha)}{\sigma(u-\bar{\alpha})}\right\}^{1/n}\left\{\frac{\sigma(u-\alpha_1)}{\sigma(u-\bar{\alpha}_1)}\right\}^{1-1/n}\left\{\frac{\sigma(u-\beta)}{\sigma(u-\bar{\beta})}\right\}\exp(2\eta_2 u), \tag{35}$$

or by applying (20),

$$dW/dz = K/\{[P(u-\alpha)-e_2]^{1/2n}[P(u-\alpha_1)-e_2]^{(n-1)/2n}[P(u-\beta)-e_2]^{\frac{1}{2}}\}, \tag{36}$$

where K_0 and δ are real constants and

$$K = \frac{K_0}{\sigma^2(\omega_2)} \exp\left[\eta_2\left(\frac{\alpha}{n}+\frac{n-1}{n}\alpha_1+\beta\right)+i\delta\right]. \tag{37}$$

From (36), we see that dW/dz has the required periods 2 and $2\omega_2$ and, by the same arguments as for the flat plate, that the wedge is a stream surface.

The function $z(u)$ is now given by

$$z(u) = \int_\alpha^u G(u)\,du, \tag{38}$$

where $G(u) = (dW/du)\,(dW/dz)^{-1}$ is given by

$$G(u) = \frac{kU}{K}[Q-P(u-\gamma;2,\omega_2)]\,[P(u-\alpha)-e_2]^{1/2n}\,[P(u-\alpha_1)-e_2]^{(n-1)/2n} \times [P(u-\beta)-e_2]^{\frac{1}{2}}. \tag{39}$$

Application to (35) of the condition of constant velocity λ along the free streamlines L_1 and L_2 again yields the result

$$\lambda = K_0. \tag{40}$$

The Taylor expansion of dW/dz in (36) about $u = \gamma$ gives

$$dW/dz \simeq K\{[P(\gamma-\alpha)-e_2]^{1/2n}\,[P(\gamma-\alpha_1)-e_2]^{(n-1)/2n}\,[P(\gamma-\beta)-e_2]^{\frac{1}{2}}\}^{-1} \times\left\{1-\frac{u-\gamma}{2n}\left[\frac{P'(1-a)}{P(1-a)-e_2}+\frac{(n-1)\,P'(1-a_1)}{P(1-a_1)-e_2}+\frac{nP'(1-b)}{P(1-b)-e_2}\right]\right\}. \tag{41}$$

Comparison with the asymptotic form of dW/dz in (10) yields

$$i\delta+n^{-1}\eta_2[a+(n-1)\,a_1+nb] = 0 \tag{42}$$

and, on applying (37) and (24),

$$K = -K_0[2e_1^2+5e_1e_2+2e_2^2]^{\frac{1}{2}} = U[P(1-a)-e_2]^{1/2n}\,[P(1-a_1)-e_2]^{(n-1)/2n}\,[P(1-b)-e_2]^{\frac{1}{2}} \tag{43}$$

and

$$\frac{P'(1-a)}{P(1-a)-e_2}+\frac{(n-1)\,P'(1-a_1)}{P(1-a_1)-e_2}+\frac{nP'(1-b)}{P(1-b)-e_2} = 0. \tag{44}$$

The condition $z(u+2) = z(u)$ gives, as for the flat plate,

$$\int_{\alpha_1-2}^{\alpha} G(u)\,du = 0, \quad \int_\alpha^{\alpha_1} G(u)\,du = 0, \tag{45a,b}$$

in which the path of integration is that indicated in (29*a*, *b*). Finally, the condition that the side of the wedge AE be of unit length yields the equation

$$\int_\alpha^\epsilon G(u)\,du = e^{i\pi/n}. \tag{46}$$

In summary, the velocity potential is given parametrically by (13), (35), (38) and (39). For evaluating the five constants ω_2, k, a, a_1 and b, we have the four equations (44), (45*a*, *b*) and (46). The results for the circulation and the stream function of the free streamlines are identical with those for the flat plate, given

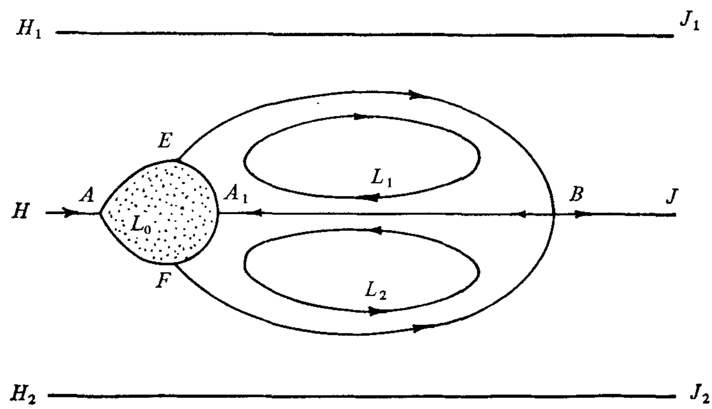

FIGURE 9. Lavrentiev model with confining walls.

in (31) and (33). The drag on the wedge, obtained in the same manner as for the flat plate, now becomes

$$D = \rho \sin\frac{\pi}{n}\left[\left|\frac{dW}{dz}\right|_E^2 - \int_\alpha^e \left|\frac{dW}{dz}\right|\frac{dW}{du}\,du\right], \tag{47}$$

where dW/dz and dW/du are given in (36) and (12), respectively.

8. The cascade problem

When the present wake model is placed symmetrically between side walls a distance d apart, the problem may be treated as a cascade of the wake flow; see Sedov (1965). We shall treat only the case of the normal flat plate; the case of wedges may be derived similarly (Lin 1970). Since the general approach to this problem is similar to that for the unbounded wake problem, only the aspects pertinent to the cascade problem will be emphasized.

8.1. *Formulation of problem*

Let L_0 represent a symmetric obstacle symmetrically situated between walls $H_1 J_1$ and $H_2 J_2$ a distance d apart, let L_1 and L_2 represent the two free streamlines and let L_3 represent the central streamline $H_1 AEA_1 BJ$, along which $\psi = 0$ (see figure 9). The discharge in the channel is then Ud, where U is the velocity of the incident uniform stream in the x direction. Here H and J represent points at $+\infty$ and $-\infty$ respectively.

By the theorem of canonical mappings, this region can be mapped into an annular region between concentric circles representing L_1 and L_2, with L_3 and HJ mapped into slits lying on a third concentric circle, representing the streamline $\psi = 0$. As in the case without walls, the Schwarz reflexion principle requires that $r_3^2 = r_1 r_2$, where r_1 is the radius of L_1, r_2 that of L_2 and r_3 that of the circle HAA_1BJ in the ξ plane.

This annular region is again transformed into a rectangular one in the parametric (u) plane by the logarithmic transformation (2). The points B, J, H, A,

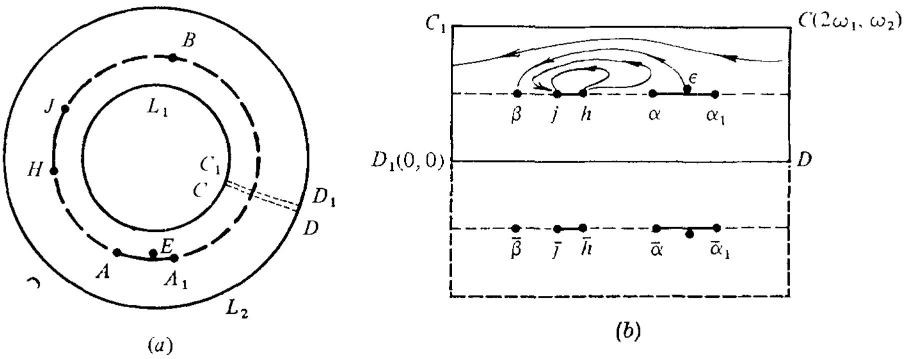

FIGURE 10. (a) ξ plane and (b) u plane for the cascade problem.

E and A_1 in the z plane are mapped into the points $\beta, j, h, \alpha, \epsilon$ and α_1 in the u plane. We also impose the condition that EE_1 and DD_1 be constant-pressure streamlines. Then, by the same arguments as were used in the case without walls, we may again establish the periodicities

$$z(u+2\omega_1) = z(u), \quad W(u+2\omega_1) = W(u),$$
$$\frac{dW}{du}(u+\omega_2) = \frac{dW}{du}(u+2\omega_1) = \frac{dW}{du}(u),$$
$$\frac{dW}{du}(u+2\omega_2) = \frac{dW}{du}(u+2\omega_1) = \frac{dW}{du}(u).$$

The transformation of the cascade flow in the z plane into the u plane requires that the discharge Ud flowing from H to J be preserved as a flow from a source at j to a sink at h of strength $Ud/2\pi$, as sketched in figure 10. Here the streamlines H_1J_1 and H_2J_2 map into the line segment JH in the u plane. Then dW/du has simple poles at h and j, and hence it is an elliptic function expressible in terms of the Weierstrass zeta function:

$$dW/du = (Ud/2\pi)[\zeta(u-h)-\zeta(u-j)+R], \tag{48}$$

where R is a constant. As in the case without walls, ϵ and β are zeros of dW/du and hence we obtain for R the real quantity

$$R = \zeta(\beta-j)-\zeta(\beta-h). \tag{49}$$

The relation between the zeros and poles of an elliptic function gives

$$h+j = \beta+\epsilon, \quad h_r+j_r = b+e, \tag{50}$$

where h_r, j_r, b and e are the real parts of h, j, β and ϵ respectively.

Equations (48) may be integrated in terms of the sigma function

$$\sigma(u) = \sigma(u; 2\omega_1, \omega_2)$$

since $\zeta(u) = \sigma'(u)/\sigma(u)$. This yields

$$W(u) = \frac{Ud}{2\pi}\left[\ln\frac{\sigma(u-h)}{\sigma(u-j)}+R\left(u-\frac{\omega_2}{2}\right)\right], \tag{51}$$

in which the constant of integration has been evaluated from the condition that $\psi = 0$ when $u = \alpha$.

The form of dW/dz is identical to that for the case without walls, since the nature of the zeros and singularities is not affected by the presence of the walls. Hence (18), (18a) and (19) remain valid, but with C replaced by C', and so does the proof that the flat plate is a streamline. The function $z(u)$ is then given by

$$z(u) = \int_{\alpha}^{u} F_1(u)\,du, \quad F_1(u) = \frac{dW}{du}\bigg/\frac{dW}{dz}, \tag{52}$$

where dW/dz and dW/du are given by (18a) and (48). The condition that L_1 and L_2 be free streamlines again yields the result that C_0 in (18) and (19) is the magnitude of the velocity along these streamlines.

8.2. *Determination of parameters*

We shall first exploit the three degrees of freedom in a conformal mapping to make the following choices:

$$\left.\begin{aligned} &(a) \quad u(D_1) = (0,0),\\ &(b) \quad \omega_1 = 1, \quad \text{or} \quad u(D) = (2,0),\\ &(c) \quad h_r + j_r = 2. \end{aligned}\right\} \tag{53}$$

The last condition implies that j and h, as well as ϵ and β, are symmetrically located with respect to the point $1 + \tfrac{1}{2}\omega_2$, the centre of the period rectangle. The remaining parameters will be determined by the following conditions.

Velocity at infinity. The condition that, at $z = +\infty$, dW/dz is real and given by $dW/dz = U$ yields, from (18a), the same results as before, (23) and (25), but with the latter equation in the form

$$C' = -C_0[2e_1^2 + 5e_1e_2 + 2e_2^2]^{\frac{1}{2}} = U\Pi(h). \tag{54}$$

Since $dW/dz = U$ at $z = -\infty$, we also have

$$\Pi(h) = \Pi(j). \tag{55}$$

We observe that (26) is the limiting form of (55) as $d \to \infty$.

Periodicity of $z(u)$. By the same procedure as in the previous case, we now obtain the pair of equations

$$⨍_{\alpha_1 - 2}^{\alpha} F_1(u)\,du = 0, \quad \int_{\alpha}^{\alpha_1} F_1(u)\,du = 0, \tag{56a,b}$$

where
$$F_1(u) = (Ud/2\pi C')\,[\zeta(u-h) - \zeta(u-j) + R]\,\Pi(u) \tag{57}$$

and the paths of integration extend along the streamline $\beta\alpha$. The symbol $⨍$ indicates that the Cauchy principal values are to be taken at the points h and j. The residues $\Pi(h)$ and $\Pi(j)$ contributed by the integrals around the small semicircles about h and j cancel each other, by (55).

Width of the flat plate. This condition yields

$$\int_{\alpha}^{\epsilon} F_1(u)\,du = i. \tag{58}$$

8.3. *Summary of equations*

For a flat plate in a channel, the complex potential has been expressed in the parametric form

$$W(u) = \frac{Ud}{2\pi}\left[\ln\frac{\sigma(u-h)}{\sigma(u-j)} + R(u-\tfrac{1}{2}\omega_2)\right], \tag{51}$$

$$z(u) = \int_a^u F_1(u)\,du, \tag{52}$$

$$F_1(u) = \frac{Ud}{2\pi C'}\left[\zeta(u-h)-\zeta(u-j)+R\right]\Pi(u), \tag{57}$$

$$R = \zeta(\beta-j)-\zeta(\beta-h), \quad C' = U\Pi(h). \qquad (49),(54)$$

For determining the six constants ω_2, a, a_1, b, j_r and h_r, we have the following five equations:

$$h_r+j_r = 2, \quad \Pi(j) = \Pi(h), \qquad (53),(55)$$

$$\int_{a_1-2}^{a} F_1(u)\,du = 0, \quad \int_a^{a_1} F_1(u)\,du = 0, \qquad (56a,b)$$

$$\int_a^{e} F_1(u)\,du = i. \tag{58}$$

Hence there exists a one-parameter family of solutions.

8.4. *Some flow characteristics*

We can now derive expressions for the circulation and stream function of the free streamlines and for the drag on the flat plate. We have, from (51),

$$\begin{aligned} W(u+2) &= [Ud/2\pi]\{\ln[\sigma(u-h+2)/\sigma(u-j+2)] + R(u-\tfrac{1}{2}\omega_2+2)\} \\ &= W(u)-(Ud/2\pi)(h-j)+2R, \quad \eta_1 = \zeta(1). \end{aligned}$$

The circulation Γ is then

$$\Gamma = -(2Ud/\pi)(h-j)+2R. \tag{59}$$

We also have, from (51),

$$W(u+\omega_2) = W(u) - Ud(h-j)\,\eta_2/\pi + R\omega_2, \quad \eta_2 = \zeta(\tfrac{1}{2}\omega_2).$$

The stream function Ψ_0 on the free streamline C_1C is then

$$\Psi_0 = iUd(h-j)\,\eta_2/2\pi + \tfrac{1}{2}R\omega_2. \tag{60}$$

Finally, the drag D on the flat plate is again given by (34), but with the complex potential W of (51).

9. Numerical results

Definitions of the *Pe* function, the sigma function and the zeta function in terms of double series are suitable for analytical purposes but are clumsy for computations. We have taken advantage of the Jacobi theta functions and some similar, rapidly converging series in evaluating these elliptic functions.

ω_2	Γ	L
0·1	24·42	14·35
0·3	9·70	6·00
0·4	8·19	5·26

TABLE 1

Some results of the calculations of flows past a flat plate are given in table 1. Here Γ represents the circulation around a free streamline, non-dimensionalized in terms of the free-stream velocity and the half-width of the plate. This indicates the total strength of the vorticity within the closed streamline. The quantity L denotes the length of the separation bubble.

These, and some additional results given by Lin (1970), were obtained by a procedure which is believed to be less efficient than the one indicated in § 6.3. Furthermore, without a quantitative relation between the free parameter and the Reynolds number, the computed characteristics of the family of wake bubbles are of limited interest. It is planned to undertake the calculation of a more complete set of characteristics in conjunction with the procedure for relating the present wake model to viscous effects described in the next section.

10. Connexion with viscous effects

We shall now consider the relation between a solution of the irrotational problem for a particular value Γ of the circulation about a free streamline within the separation bubble and the Reynolds number of a 'real' flow. In the real flow, the no-slip condition is satisfied on the upstream face of the blunt body (*FAE* in figure 3), on which a boundary layer, computable from the irrotational-flow solution, is present. The subsequent diffusion and convection of the vorticity in the space between *AB* and *CD* (figure 2) cannot be readily determined, but we shall suppose that a reasonable approximation to the distribution of vorticity in this region will suffice, and can be assumed. Within the separation bubble, viscous effects, such as the no-slip condition on the surface of the body within the separation bubble, will be ignored under the assumption that the vorticity generated by viscosity within the bubble is concentrated as vortex sheets on the pair of internal free streamlines.

The 'real' flow field is now seen to be generated by the following mechanisms: a uniform stream in the $+x$ direction, the known vorticity in the boundary layer and the assumed vorticity between the separation bubble and the outer boundary of the wake, a vortex sheet on the surface of the body within the separation bubble (with strength given by the velocity distribution on that surface, calculated from the irrotational Lavrentiev model) and the vortex sheets on the free-streamline contours. In this selection of the flow-generating mechanisms, the velocity within the blunt body has been taken to be zero. Because of the no-slip condition on the upstream face of the body, there is then no discontinuity in the normal component of the velocity across this surface, so that a source distribution on this surface is unnecessary. A vortex sheet is required on the back face because of the discontinuity in the tangential component of the velocity. Thus it is possible to generate the entire disturbance flow field by means of vorticity alone, with the velocity at a point computed by means of the Biot–Savart law.

The boundary layer on the upstream surface of the body, calculated from the pressure gradients of the irrotational flow for a particular value of the circulation Γ about a free streamline, will have different vorticity distributions as the Reynolds number is varied. Consequently, the velocity at a point, computed from the uniform stream and the aforementioned distributions of vorticity, will also vary with the Reynolds number. The condition that the point A on the back face (figure 3) remains a stagnation point then gives a relation between the circulation and the Reynolds number. This point, rather than a point on the separation streamline, is selected for obtaining this relation because it is as far away as possible from the assumed part of the vorticity distribution within the zone between the separation streamline and the wake boundary, thus minimizing the error due to this assumption.

11. Summary

We have considered some general physical features of a near wake. In particular we note that the dividing streamline of a wake bubble must reattach at a stagnation point and form the closure of the wake bubble. In comparison with others, Lavrentiev's wake model is seen to possess features that would best simulate the closure of a near wake.

Solutions of Lavrentiev's wake model for a flat plate and wedges are derived by conformal mapping. Analysis and solution are conducted on a rectangular parametric (u) plane in which the forms of the solutions are indicated by the double periodicities of complex velocities. A one-parameter family of solutions is developed. The undetermined parameter provides the link between the model and the conditions of the real wake.

To carry out a complete computation, numerical integration on the complex plane is necessary. Definitions, in terms of double series, of the *Pe* function, the sigma function and the zeta function are suitable for performing the analysis, but clumsy for computational purposes. Consequently, it is advantageous to use the Jacobi theta functions and some similar, rapidly converging series in evaluating these elliptic functions (Whittaker & Watson 1960, p. 462). A method of successive approximation has been developed for solving a set of simultaneous equations for three of four constants, the fourth serving as the free parameter of the solution. Associated flow parameters, such as the stream function and the circulation, may be easily computed.

We note that a fruitful computation must be accompanied by a well-designed experimental study of a quasi-steady near wake; so far only a few computations have been performed (Lin 1970). A preliminary experimental study has been conducted to investigate features of the near wake which are pertinent to the Lavrentiev wake model (Lin & Sha 1975). With the solution for the cascade problem available, it is conceivable that the wall effect could be inferred from the results of the present study after the relation of the model with viscous effects has been established in accordance with the procedure proposed here.

This work was supported by the Office of Naval Research under Contract N00014-76-C-00012.

REFERENCES

ABRAMOWITZ, M. & STEGUN, I. E. 1964 *Handbook of Mathematical Functions*. Washington: Nat. Bur. Stand.

ACRIVOS, A., LEAL, G., SNOWDEN, D. D. & PAN, F. 1968 Further experiments on steady separated flows past bluff objects. *J. Fluid Mech.* **34**, 25–48.

ACRIVOS, A., SNOWDEN, D. D., GROVE, A. S. & PETERSEN, E. E. 1965 The steady separated flow past a circular cylinder at large Reynolds numbers. *J. Fluid Mech.* **21**, 737–60.

ARIE, M. & ROUSE, H. 1956 Experiments on two-dimensional flow over a normal wall. *J. Fluid Mech.* **1**, 129–41.

BATCHELOR, G. K. 1956 A proposal concerning laminar wakes behind bluff bodies at large Reynolds numbers. *J. Fluid Mech.* **1**, 388–98.

DUTTA, M. & DEBNATH, L. 1965 *Theory of Elliptic and Associated Functions*. Calcutta: The World Press Private, Ltd.

GROVE, A. S., SHAIR, F. H., PETERSEN, E. E. & ACRIVOS, A. 1964 An experimental investigation of the steady separated flows past a circular cylinder. *J. Fluid Mech.* **19**, 60–80.

LANDWEBER, L. 1970 A note on blockage effect. In *Jubilee Memorial W.P.A. Van Lammeren Volume*, pp. 49–51. Netherlands Ship Model Basin, Wageningen.

LAVRENTIEV, M. A. 1962 *Variational Methods for Boundary Value Problems for Systems of Elliptic Functions*. Noordhoff.

LIGHTHILL, M. J. 1960 *Fourier Analysis and Generalised Functions*. Cambridge University Press.

LIN, A. 1966 Effect of channel walls on base pressure and flow of a blunt body. M.S. thesis, University of Iowa, Iowa City.

LIN, A. 1970 A free-streamline model of two-dimensional wake. Ph.D. dissertation, University of Iowa, Iowa City.

LIN, A. & SHA, P. Y. 1975 Some flow characteristics in the vicinity of reattachment point behind a flat plate. *Proc. 2nd U.S. Nat. Con. Wind Engng. Res.*, vol. IV–24, pp. 1–3.

NEHARI, Z. 1952 *Conformal Mapping*. McGraw-Hill.

SEDOV, L. I. 1965 *Two Dimensional Problems in Hydrodynamics and Aerodynamics*. Wiley.

WHITTAKER, E. T. & WATSON, G. N. 1950 *A Course of Modern Analysis*. Cambridge University Press.

WU, T. Y. 1972 Cavity and wake flows. *Ann. Rev. Fluid Mech.* **4**, 243–84.

WU, T. Y., WHITNEY, A. K. & BRENNAN, C. 1971 Cavity-flow wall effects and correction rules. *J. Fluid Mech.* **49**, 223–56.